Journal of Advanced Research 50 (2023) 55–68

Contents lists available at ScienceDirect

Journal of Advanced Research

journal homepage: www.elsevier.com/locate/jare

Original Article

SAP deficiency aggravates periodontitis possibly via C5a-C5aR signaling-mediated defective macrophage phagocytosis of *Porphyromonas gingivalis*

Liping Wang [a,1], Dongliang Liang [a,1], Yinyin Huang [a,1], Yunxin Chen [a], Xiaocong Yang [a], Zhijun Huang [a], Yiqin Jiang [a], Hanfu Su [a], Lijing Wang [a,b,*], Janak L. Pathak [a,*], Linhu Ge [a,*]

[a] *Affiliated Stomatology Hospital of Guangzhou Medical University, Guangdong Engineering Research Center of Oral Restoration and Reconstruction, Guangzhou Key Laboratory of Basic and Applied Research of Oral Regenerative Medicine, Guangzhou, Guangdong 510182, China*
[b] *Vascular Biology Research Institute, School of Life Sciences and Biopharmaceutics, Guangdong Pharmaceutical University, Guangzhou, China*

HIGHLIGHTS

- Macrophage-specific SAP is the main source of the elevated level of periodontal SAP during periodontitis.
- SAP deficiency exacerbated periodontitis, inflammation, and infiltration of M1-type proinflammatory macrophages in the periodontium.
- SAP deficiency resulted in a higher abundance of Porphyromonas genus in the oral cavity of periodontitis mice.
- SAP depleted macrophages induced C5a release from *P. gingivalis* and inhibited macrophage phagocytosis of *P. gingivalis* via C5a-C5aR signaling.
- A higher abundance of *Porphyromonas* during SAP deficiency could promote M1 macrophage polarization and inflammation in the periodontium.

GRAPHICAL ABSTRACT

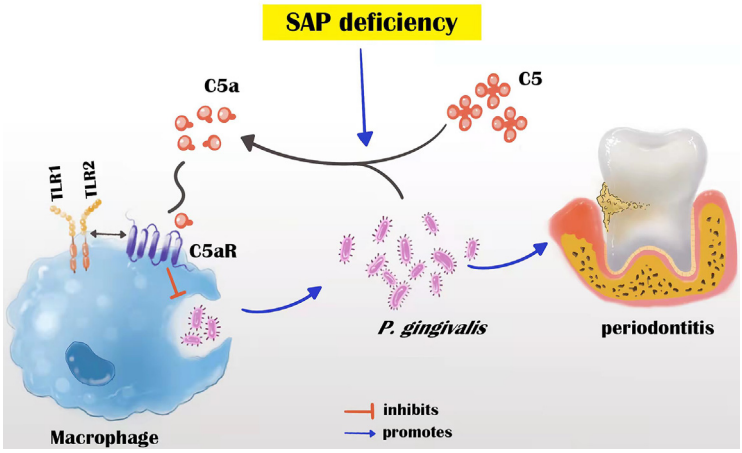

ARTICLE INFO

Article history:
Received 5 July 2022
Revised 4 October 2022
Accepted 4 October 2022
Available online 12 October 2022

ABSTRACT

Introduction: Serum amyloid P component (SAP) regulates the innate immune system and microbial diseases. Periodontitis is an inflammatory oral disease developed by the host immune system's interaction with the dysbiotic oral microbiome, thereby SAP could play a role in periodontitis pathogenicity.
Objectives: To investigate the role of SAP in oral microbiome modulation and peridontitis pathogenicity.

Abbreviations: SAP, Serum amyloid P component; PVDF, Polyvinylidene fluoride; FACS, Fluorescence-activated cell sorting; OTU, Operational taxonomic units; LDA, Linear discriminant analysis.

Peer review under responsibility of Cairo University.

* Corresponding authors at: Affiliated Stomatology Hospital of Guangzhou Medical University, Guangdong Engineering Research Center of Oral Restoration and Reconstruction, Guangzhou Key Laboratory of Basic and Applied Research of Oral Regenerative Medicine, Guangzhou, Guangdong 510182, China (J.L. Pathak).
E-mail addresses: 2018991265@gzhmu.edu.cn (L. Wang), J.pathak@gzhmu.edu.cn (J.L. Pathak), gelinhu@yeah.net (L. Ge).
[1] These authors contributed equally and share the first authorship.

https://doi.org/10.1016/j.jare.2022.10.003

Keywords:
Serum amyloid P component
Periodontitis
Macrophages
Porphyromonas gingivalis
C5a-C5aR signaling

Methods: In this study, wildtype and SAP-knockout (KO) mice were used. Ligature-based periodontitis was developed in mice. Oral microbiome diversity was analyzed by 16 s rRNA sequencing. Macrophages and *Porphyromonas gingivalis (P. gingivalis)* co-culture system analyzed the effect of SAP in macrophage phagocytosis of *P. gingivalis.*
Results: The level of SAP was upregulated in the periodontitis-affected periodontium of humans and mice but not in the liver and blood circulation. Periodontal macrophages were the key source of upregulated SAP in periodontitis. SAP-KO aggravated periodontal inflammation, periodontitis, and a higher number of M1-type inflammatory macrophage infiltration in the periodontium. The oral microbiome of SAP-KO periodontitis mice was altered with a higher abundance of *Porphyromonas* at the genus level. SAP-KO macrophages showed compromised phagocytosis of *P. gingivalis* in the co-culture system. Co-culture of SAP-KO macrophages and *P. gingivalis* induced the C5a expression and exogenous SAP treatment nullified this effect. Exogenous recombinant SAP treatment did not affect *P. gingivalis* growth and opsonization. PMX205, an antagonist of C5a, treatment robustly enhanced *P. gingivalis* phagocytosis by SAP-KO macrophages, indicating the involvement of the C5a-C5aR signaling in the compromised *P. gingivalis* phagocytosis by SAP-KO macrophages.
Conclusion: SAP deficiency aggravates periodontitis possibly via C5a-C5aR signaling-mediated defective macrophage phagocytosis of *P. gingivalis*. A higher abundance of *P. gingivalis* during SAP deficiency could promote M1 macrophage polarization and periodontitis. This finding suggests the possible protecting role of elevated levels of periodontal SAP against periodontitis progression.

Introduction

Periodontitis, a highly prevalent disease of the oral cavity, causes tooth loss and is associated with systemic diseases including hypertension, cardiac diseases, and neuronal diseases [1]. Many studies have reported periodontitis as a complex inflammatory disease with several etiologic and contributing factors [2,3]. Recent studies based on oral microbiome analysis revealed microbiome dysbiosis and host susceptibility as key processes of periodontitis pathogenicity [2,3]. The oral microbiota is composed of more than 700 bacterial species, which maintains microbiome homeostasis and is usually non-pathogenic in healthy individuals [4]. However, according to the "Keystone Pathogen" hypothesis, the low abundance of microbial pathogens has the potential to induce microbiome dysbiosis [5]. *Porphyromonas gingivalis (P. gingivalis)* is a gram-negative anaerobic bacteria that is a proven periodontitis Keystone Pathogen [4]. Furthermore, *P. gingivalis* interferes with host immunity, causes oral microecological disorders, and promotes the occurrence and development of periodontitis [6].

SAP (also known as PTX2) is a pentraxin protein present in the majority of amyloid deposits that was first isolated in serum [7]. According to RNA-seq databases and proteomics, SAP is mainly produced in the liver [8,9]. The human serum level of SAP is approximately 30 mg/L [10]. SAP level goes up to 20-fold in mice during bacterial infection and tissue injury [11,12]. As the soluble pattern recognition molecule, SAP plays an important role in the innate immune system [12]. During bacterial infections, SAP exerts differential effects on different microbes. SAP increases virulence during infection of *Escherichia coli*, *Neisseria meningitidis*, *Streptococcus pyogenes*, or fungi [13,14]. In contrast, SAP binds to teichoic acid-deficient *ΔtagO* mutant of *Staphylococcus aureus* to promote the phagocytosis of this pathogen [15]. The higher expression of SAP has been reported in biopsies of established periodontitis lesions and non-destructive marginal gingivitis in humans by immunohistochemistry [16]. However, the effect of SAP on periodontitis-related pathogens and host immune cells' function is still unclear.

Interaction between pathogenic bacteria and host immune cells is a key process of periodontitis progression. Macrophages are major immune cells of innate immunity [17] and participate in periodontitis pathogenesis by regulating periodontal biofilm, activating adaptive immunity, and mediating the absorption and repair of alveolar bone [18,19]. Macrophages are classified as pro-inflammatory macrophages (M1) and anti-inflammatory macrophages (M2) according to their immunomodulatory functions. Moreover, SAP regulates macrophage polarization-related immune regulation [20–22]. However, the periodontal SAP level in periodontitis and its role in disease progression are still unknown. Pathogenic bacteria invade periodontal tissue and secrete gingival protease that activates the C5 complement system and releases C5a fragments [23,24]. With the participation of the TLR2/1 complex, C5a inhibits the macrophage phagocytosis of pathogens and causes microecological disorders, which further regulate periodontitis pathogenicity [25,26]. However, the role of SAP in C5a release from pathogenic bacteria during periodontitis should be further investigated.

This study aimed to analyze: (1) the expression pattern of SAP in the periodontium and its role in periodontitis pathogenicity; (2) the effect of SAP on macrophage polarization and oral microbiome abundance during periodontitis; and (3) the role of SAP in the regulation of macrophage phagocytosis of pathogenic bacteria and the underlying mechanisms. We found the increased SAP level in periodontitis periodontium and macrophages were the key source of the upregulated SAP. SAP-knockout (KO) aggravated periodontitis and increased the periodontium inflammation via infiltration of M1 macrophage. A higher abundance of *Porphyromonas* at the genus level was observed in the oral cavity of SAP-KO periodontitis mice. SAP deficiency in macrophages aggravated periodontitis pathogenicity and inhibited phagocytosis of *P. gingivalis* in vitro via upregulating C5a-C5aR signaling, suggesting the possible protecting role of elevated levels of periodontal SAP against periodontitis progression..

Materials and methods

Human sample collection

periodontitis patients and healthy controls (18 in each group) visiting the Affiliated Stomatology Hospital of Guangzhou Medical University (November 2019 to November 2021) were recruited. Radiography and clinical examination confirmed the healthy controls or periodontitis patients. Human gingiva of healthy controls was obtained during impacted tooth extraction. Diseased gingiva

was obtained from patients during surgical treatment for periodontitis. The expression of SAP protein was detected by enzyme-linked immunosorbent assay (ELISA). Table S1 summarizes the clinical and demographic characteristics of patients and healthy controls. The Medical Ethics Committee of Affiliated Stomatology Hospital of Guangzhou Medical University approved the patient's sample-related studies (approval number: KY2019032). Each participant provided informed consent.

Cell culture

Murine pre-osteoblast cell line MC3T3-E1 and mouse gingival epithelial cells (GECs) were purchased from Procell Life Science&Technology Co., ltd (Wuhan, China). Both MC3T3-E1 and GECs were cultured in standard culture medium (DMEM medium supplemented with 10 % FBS and 1 % antibiotics (streptomycin 100 U/mL, penicillin 100 U/mL)). Mice bone marrow-derived macrophages (BMDM) were harvested and cultured [27].

Animals

C57/BL6 wildtype mice were obtained from Guangdong Medical Animal Experiment Center (Guangdong, China, permit number. SCXK2018-0002). SAP-KO mice were obtained from Prof. Lijing Wang's lab, Vascular Biology Research Institute, School of Life Sciences and Biopharmaceutics, Guangdong Pharmaceutical University, Guangzhou 510006, China. SAP-KO mice construction procedure and genetic verification are provided in Supplementary data (Fig. S1). This study used eight weeks old male mice with 22 $\sim$ 25 g body weight. The Institutional Laboratory Animal Care and Use Committee of Guangzhou Medical University approved this study (GY2020-004).

Ligature-based periodontitis development in mice

Ligature-based mouse periodontitis model is widely used for periodontitis research. Although this model uses a mechanical way, the bacterial accumulation around the ligature mainly progresses the periodontitis [28]. Moreover, this model allows analysis of most aspects of periodontitis, including bacterial interactions and dysbiosis, periodontal inflammatory responses, and bone biology [29]. The periodontitis model was established in wildtype mice and SAP-KO mice by silk ligature method [28]. The mice were sacrificed by cervical dislocation 7 days after ligature. The mice maxilla were collected to analyze the periodontitis pathogenicity.

Micro-CT analysis

The maxilla tissues were fixed in 4 % paraformaldehyde at room temperature for 24 h. The fixed maxilla tissues were scanned by SkyScan1172 (Bruker-Micro-CT, Kontich, Belgium) using 60 kV device voltage 60, 100 μA current, 10 μm scanning volume voxel resolution. The NRECON and CTVOX software was used for the 3D reconstruction of the scanned images. The bone height of the maxillary second molar was measured by SkyScan Dataviewer software. The distances from the cementum enamel junction to the alveolar bone crest (CEJ-ABC) distances were measured at 6 fixed palatal sites [30]. Each site was measured three times, and the average of 6 sites represented the bone resorption height.

Histological evaluation

The histological tissue sections of the maxilla were stained with Hematoxylin and eosin (H&E) and tartrate-resistant acid phosphatase (TRAP) staining [30]. Images of stained tissue sections were taken (DM4000B-LED/DFC450, Leica, Wetzlar, Germany). The CEJ-ABC distance and the number of multinucleated osteoclasts were analyzed.

Immunohistochemistry

Tissue sections were incubated with sodium citrate antigenic repair fluid (EDTA, Solarbio) in a pressure cooker for 8 min to retrieve the antigen. To block endogenous peroxidase, the slides were soaked in a box containing 3 % H_2O_2-methanol solution and placed in a drying oven at 37℃ for 30 min. Bovine serum albumin (BSA, 10 %) blocked tissue sections were incubated with primary antibodies: anti-SAP (GTX55792, Gene Tex, USA), anti-CD34 (AB81289, Abcam, Cambridge, UK), anti-CD45 (20103–1-AP, ProteinTech, US), anti-F4/80 (70076, CST, US) or isotype controls for overnight at 4 °C. Corresponding secondary antibodies anti-rabbit/anti-mouse (SolelyBio, Beijing, China) were used. The diaminobenzidine chromogen (Cell Signaling Technology, MA, USA) was immunolabeled (Cell Signaling Technology, MA, USA) and counterstained with Mayer's hematoxylin. The tissue sections' images were taken under a light microscope and immunostained cells were counted.

Immunofluorescence staining

BMDM (2×10^5) were seeded in a round coverslip that fits in 12-well plates with or without Pg-LPS (Invivogen, USA) treatment for 24 h. Cultures were washed with PBS and fixed with 4 % paraformaldehyde for 15 min. And, 0.3 %Triton X-100 (prepared with 1 × PBS) treatment was performed to permeabilize the cells. Incubation with normal goat serum (New Zealand origin, Gibco) at room temperature for 30 min blocked the cells before staining. BMDM or tissues section were incubated with the primary antibody F4/80 (1:100 Invitrogen, MA5-32846, USA), SAP (1:100, GTX55792, GeneTex, USA) in a wet box at 4 °C overnight. After 3 times washing with PBS, samples were incubated with fluorescent-labeled secondary antibodies (1:200, AMCA, Earthox, USA) in a wet box at 37 °C for 1 h. The nucleus was stained with Hoechst (Beyotime, Hoechst33342) in dark conditions for 5 min. Fluorescence mages were taken (LEICATCSSP8) and quantified using Image J.

Immunofluorescence staining visualized the BMDM phagocytosis of *P. gingivalis*. In brief, *P. gingivalis* were counted and labeled with FITC (Yeasen Biotechnology, 60514ES60, Shanghai, China). *P. gingivalis* with a multiplicity of infection (MOI) of 100:1 was used to infect BMDM. After co-culturing for 30 min, 1 h, and 2 h respectively, the culture medium was discarded, and immunofluorescence staining was performed using primary antibody F4/80 (D4C8V, 1:100, Cell Signaling Technology, USA) as described above in this subsection.

RT- qPCR

Maxillary tissue total RNA was isolated as described previously [30]. The total RNA from MC3T3-E1 cells, GECs, and BMDM was isolated using Trizol. NanoDrop spectrophotometer (NanoDrop2000, Wilmington, DE, USA) analyzed the concentration and quality of RNA. Reverse transcription of total RNA was performed using Takara PrimeScriptTM RT Master Mix. RT-qPCR for the specific gene was performed using Takara TB-Green Premix Ex Taq in the LightCycler RT-qPCR system (LC-480 II, Roche, Switzerland). The primers used in this study can be found in Table S2.

Western blot analysis

MC3T3-E1 cells, gingival epithelial cells, and BMDM were seeded in 6-well plates (5×10^5 cells/well), with or without Pg-LPS (Invivogen, USA) treatment for 24 h. The cell lysate was prepared in a lysate solution (P0013B, Beyotime, China). The periodontal tissue lysate was prepared and protein concentration was analyzed as described previously [30]. Total protein (20 μg) was separated by 15 % SDS-PAGE and transferred onto polyvinylidene fluoride (PVDF) membranes (EMD Millipore, Billerica, MA, USA). The membranes were blocked with blocking buffer (P0260, QuickBlock™, Beyotime, China) at room temperature for 30 min and incubated with the primary antibody SAP (1:1000, GTX55792, GeneTex, USA) at 4 °C overnight. After washing 3 times with PBST, the membranes were incubated with horseradish enzyme-labeled secondary antibodies (1:3000, Cell Signaling Technology, 7074S, USA) at room temperature for 1 h. Membranes were washed three times with PBST. The immunoreactive protein bands were detected with an enhanced chemiluminescence detection system BLT GelView 6000 Pro (BioLight, Guangdong, China).

Flow cytometry analysis

Analysis of macrophages in periodontal tissue of mice: The cell suspension was prepared and used for fluorescence-activated cell sorting (FACS) as described previously [30]. Cells were stained with 1 μg of PE anti-mouse F4/80 (123110, BioLegend, San Diego, CA, USA) solution, FITC anti-mouse/human CD11b (101206, BioLegend, San Diego, CA, USA), PerCP/Cyanine5.5 anti-mouse CD16/32 (101324, BioLegend, San Diego, CA, USA), APC anti-mouse CD206 (141707, BioLegend, San Diego, CA, USA) or anti-rabbit IgG per 1×10^6 cells for 30 min on ice in the dark. After washing twice with PBS, the cells were resuspended in 300 μl stain buffer and transferred to a flow tube. FACS analysis was performed in FACSAria III Cell Sorter (BD Biosciences, San Jose, CA, USA).

P. gingivalis phagocytosis by macrophages: P. gingivalis was pre-labeled with FITC and added to BMDM at the ratio of 100:1, incubated at 37 ℃, 5 % CO_2 then washed in PBS 3 times. And 50 μl of trypan blue (pH-4.4, 0.125 %) was added for 2 min. Cells were stained with PE/Cyanine7 anti-mouse F4/80 (123114, BioLegend, San Diego, CA, USA) antibody. After two times washing with PBS, the cells were resuspended and sorted. The FITC positive rate of macrophages represents the phagocytosis rate.

For the experiment on whether SAP binds to *P. gingivalis* affects phagocytosis by macrophages, a recombinant SAP protein (1948-SAB-050, R&D Systems, USA) was added in *P. gingivalis culture* and incubated for 2 h to make SAP binds to *P. gingivalis*. The phagocytosis rate of *P. gingivalis* was detected by flow cytometry of wild-type macrophages. For the recovery experiment of phagocytosis, a C5a receptor peptide antagonist (B7787, APExBIO, Beijing, China) was added to *P. gingivalis* and macrophage co-culture. The phagocytosis rate of *P. gingivalis* was detected by flow cytometry of PMX205-added SAP-KO macrophages.

Analysis of spleen macrophages in mice after injection of clodronate liposomes: Immediately after sacrifice, the spleen of mice were taken and washed with PBS. The spleen was ground in a bowl to make it fully homogenized. The red blood cells were lysed and the remaining cells were centrifuged and washed with PBS 3 times. Cells were counted and analyzed for cell viability using Zombie NIRTM Fixable Viability Kit (423105, Biolegend, Beijing, China). Cells were stained with 5 μg of PE-Cy7 anti-mouse F4/80 (123114, BioLegend, San Diego, CA, USA) solution, PerCP-Cy5-5-anti-mouse CD11b (101206, BioLegend, San Diego, CA, USA). The number of macrophages was counted by flow cytometry.

Enzyme-linked immunosorbent assay (ELISA)

SAP expression: The SAP protein expression level in human and mouse periodontium, mouse serum, and liver was detected by ELISA. Human and mouse periodontal tissues lysate and mouse liver lysate serum were obtained as described previously [31]. The protein level of SAP in the human gingival lysate was analyzed using the human SAP ELISA kit (Cusabio, Wuhan, China) and in mouse periodontal tissue lysate, liver lysate, and serum was analyzed using the mouse SAP ELISA kit (SEB539Mu, Cloud-Clone Corp, Wuhan, China). Levels of IL-6, IL-1β, and TNF-α in periodontal tissue lysate were measured using the mouse ELISA Standard Kits (RayBiotech, Atlanta, USA).

C5a expression in co-culture supernatant: With or without adding the recombinant SAP protein (10 ng/ml) to the bacteria-macrophage co-culture system, the supernatantwas collected after *P. gingivalis* exposure for 30 min, 1 h, and 2 h, and centrifuged for 20 min at 1000 g. The expression level of C5a in the supernatant of co-culture was analyzed using the C5a ELISA kit (MLbio, ml1001972-C, Shanghai, China). The SAP concentration (10 ng/ml) for this experiment was chosen based on the ELISA results of SAP concentration in mouse periodontal tissue during periodontitis.

16S rRNA sequencing

Sample collection: The oral microbiome in murine models was assayed by using 16S rRNA gene sequencing. Before the experiment, wildtype and SAP-KO mice were co-housed for 1 week to maintain the consistency of the oral microbiomes. Saliva, gingival tissues, and ligature threads were collected from each mouse and stored separately. Samples were stored at −80 °C. Three samples from each mouse were sequenced and data were combined to represent the oral microbiome of each mouse. The maxillary second molars of healthy group mice were ligated 2 h before sampling (Johnson & Johnson, USA).

Microbial genomic DNA extraction and library preparation: Genomic DNA was extracted using a bacterial DNA extraction mini Kit (Mabio, China), and the purity and concentration of DNA were detected by Thermo NanoDrop One. Genomic DNA was used as a template and PCR amplification was performed using specific primers (Table S2) with barcode and TaKaRa Premix Taq® Version 2.0 (TaKaRa Biotechnology Co., Dalian, China). GeneTools Analysis Software compared the concentration of PCR products (Version4.03.05.0, SynGene). Each sample required was calculated by the equal mass principle. E.Z.N.A.® Gel Extraction Kit (Omega, USA) was used to recover PCR mixed products, and TE buffer was used to elute the target DNA fragments. NEBNext® Ultra II DNA Library Prep Kit for Illumina® (New England Biolabs, USA) standard process was used to build the library. The amplified sublibrary was sequenced by PE250.

Sequencing data analysis: Paired-end Raw Reads data filtering was performed using fastp (an ultra-fast all-in-one FASTQ preprocessor, version 0.14.1, https://github.com/OpenGene/fastp) to tailor the Raw Reads data of both ends with slippery window quality (-W4-M20). The primer was removed by cutadapt software (https://github.com/marcelm/cutadapt/) to get the quality-controlled paired-end Clean Reads. Paired-end Clean Reads splicing was performed for double-terminal sequencing data. Raw Tags sequence quality filtration was performed using fastp (an ultra-fast all-in-one FASTQ preprocessor, version 0.14.1, https://github.com/OpenGene/fastp) to conduct slippery window quality clipping (- W4-M20) to obtain effective splicing fragments. The effective data were analyzed for operational taxonomic units (OTU) clustering and species Annotation.

Microbial community analysis

R software analyzed the relative abundance of every classification group. Then, the classification groups with relative abundance above 0.01 % (default value) were selected, the top 15 (default value) were selected, and the histograms of relative abundance of species were drawn. R software was further used for cluster analysis of species abundance, the heat map of species was generated for each group at different genus levels. Selected the method of average to cluster the samples, and 30 species with higher abundance are selected from the mapping data. The usearch-alpha_div_rare (V10, https://www.drive5.com/usearch/) was used to calculate the dilution curve of the richness diversity index based on the OTU_table. The difference in alpha diversity index among groups was analyzed by the R software and the chao1 index was obtained after the Kruskal-Wallis rank-sum test to evaluate whether there was a significant difference in diversity index among different groups. Based on the OTU_table, the vegan software package of R software with bray_curtis distance algorithm was used for Beta diversity analysis-principal coordinate analysis (PCoA). And the similarity between samples was evaluated showing the natural distribution of samples under a certain distance scale. LEfSe analysis was performed based on the homogenized abundance table OTU_table of each species level, LEfse software was used to analyze the significant differences. Firstly, the significant abundance differences of species were detected by a non-parametric factorial Kruskal-Wallis (KW) sum-rank test, and then the group Wilcoxon rank-sum test judged the differences between the groups. Finally, linear discriminant analysis (LDA) reduced and evaluated the influence of each significant species (that is, LDAScore).

Culture and counting of P. Gingivalis

P. gingivalis (ATCC33277) was inoculated on a Columbia Blood Agar Plate (HuanKai Microbial, CP0160, Guangzhou, China) and cultured in a 37℃ constant anaerobic incubator (10 % H_2 + 10 % CO_2 + 80 % N_2 mixture) (ELECTROTEK, AW200SG, The United Kingdom) for 5–7 days. Single colonies were selected from the blood agar plate and inoculated in BHI (HOPEBIO, HB8297-1, Qingdao China) liquid medium supplemented with yeast extract (5 mg/mL), hemin (5 mg/mL), and vitamin K (0.5 mg/mL). When the *P. gingivalis* grew to the logarithmic phase and the absorbance value was more than 0.6, the bacteria were harvested and centrifuged at 4000 rpm and re-suspended in 5 mL PBS, 10 μl of which was continuously diluted to 1×10^{-7} and inoculated on the plate. After 5 days, the colony-forming unit was calculated, and the total number of bacteria was obtained.

FITC labeling P. Gingivalis

The FITC (Yeasen Biotechnology, 60514ES60, Shanghai, China), stock solution concentration was prepared with dimethyl sulfoxide and added to the bacterial suspension at a concentration of 10, 50, 100, 200, or 500, μg/mL respectively. After 2 h incubation, the supernatant was discarded, and the pellet was re-suspended in a cell culture medium, and stored for use.

Statistical analysis

All data were presented as mean ± standard deviation (SD). An unpaired, nonparametric Mann-Whitney test or a two-tailed unpaired *t*-test was used to determine differences between the two groups. For multiple comparisons of groups, a one-way analysis of variance (ANOVA) was performed followed by Bonferroni's multiple comparison test. Data were analyzed with GraphPad Prism 7.0 statistical software (GraphPad, San Diego, CA, United States). Values were considered significantly different if $p < 0.5$.

Results

The SAP is upregulated in periodontitis periodontium

First, we analyzed the SAP expression pattern in clinical gingival samples from periodontitis patients and healthy individuals. The SAP protein level expression in the periodontitis group was higher compared with the healthy control group (Fig. 1a). A similar level of SAP expression was observed in the serum of healthy individuals and periodontitis patients (Fig. S2a). Next, we analyzed the expression pattern of SAP in mice tissues, including, blood, liver, and periodontium. The mRNA and protein level expression of SAP in periodontitis mice periodontium was higher compared with the control group (Fig. 1b). Whereas SAP expression level was similar in serum or liver of periodontitis and control mice (Fig. 1c-1e). Our results suggested that during periodontitis, SAP is mainly upregulated in periodontium tissue, rather than in the liver. Immunohistochemistry staining and western blot detection also confirmed the higher expression of SAP in the periodontium of periodontitis mice compared with control mice (Fig. 1f, g, i, j). Western blot quantification showed a 2.1-fold higher expression of SAP in the periodontium of periodontitis mice compared with control mice (Fig. 1j). Interestingly, SAP level in liver tissue of periodontitis mice was not altered compared with control mice (Fig. S2b, c). LPS treatment induced the expression of SAP in BMDM (Fig. 1h, i, k). Immunofluorescence staining further confirmed the higher SAP expression in LPS-treated BMDM (Fig. 1l, m). Whereas SAP expression in gingival epithelial cells was reduced by treating with LPS (Fig. S3a, d, e). LPS treatment did not affect SAP expression in pre-osteoblasts (Fig. S3b, d, f). Furthermore, we also investigated the effect of LPS treatment on SAP expression by RAW264.7 murine macrophages. LPS treatment robustly induced SAP expression also in RAW264.7 cells (Fig. S3c, d, g, h, i). These results indicated macrophages as a key source of elevated SAP levels in the periodontium during periodontitis.

SAP deficiency aggravates periodontitis and inflammation in the periodontium

Periodontium of SAP-KO mice showed no expression of SAP in both healthy and periodontitis conditions (Fig. S4). Micro-CT images of the maxilla revealed that periodontitis induces more alveolar bone loss in SAP-KO mice compared with wildtype mice (Fig. 2a, b). H&E staining further confirmed the increased alveolar bone loss in SAP-KO periodontitis mice (Fig. 2c, d). The CEJ-ABC distance in SAP-KO periodontitis mice was 1.5-folds higher compared with wildtype periodontitis mice. TRAP staining results showed a higher number of multinucleated osteoclasts in the alveolar bone of SAP-KO periodontitis mice compared with wildtype periodontitis mice (Fig. 2c, e). The periodontium of SAP-KO periodontitis mice showed a higher number of micro-vasculatures and leukocyte infiltration compared with that of wildtype periodontitis mice (Fig. 2c, f, g). Moreover, The expression of pro-inflammatory cytokines was higher in the periodontium of SAP-KO periodontitis mice. Both mRNA and protein level expressions of IL-1β, IL-6, and TNF-α were higher in the periodontium of SAP-KO periodontitis mice compared with wildtype periodontitis mice (Fig. 2h ∼ m). These findings demonstrated that SAP deficiency aggravates periodontitis by upregulating inflammation and osteoclastogenic activity in periodontal tissues.

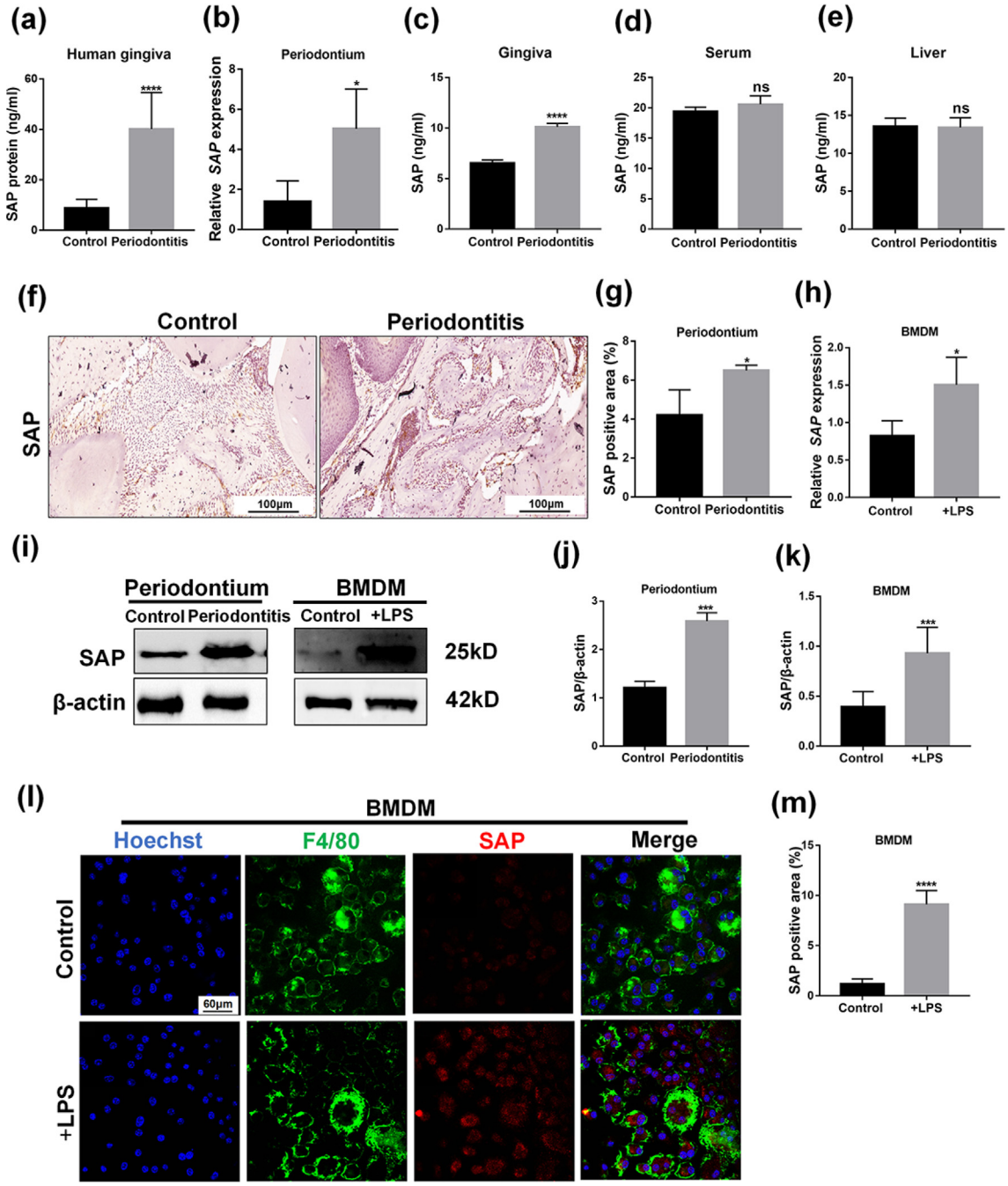

Fig. 1. The expression of SAP is upregulated in periodontitis periodontium. (a) Expression of SAP protein in gingiva tissue of healthy and periodontitis individuals (n = 18). (b) Relative SAP mRNA expression in the periodontium of control and periodontitis wildtype mice (n = 4). Expression of SAP protein in the gingiva (c), serum (d), and liver (e) of control and periodontitis wildtype mice (n = 6). (f) SAP immunohistochemistry images of control and periodontitis wildtype mice. (g) Quantification of immunohistochemistry results (n = 3). (h) Relative mRNA expression of SAP in BMDM with or without LPS treatment (n = 4). (i-k) Western blots of SAP protein expression in the periodontium of control and periodontitis wildtype mice (n = 3), as well as in BMDM with or without LPS treatment (n = 8). (l) Immunofluorescence image of BMDB with or without LPS treatment. (m) Quantification of SAP expression (n = 6). Data are presented as mean ± SD. The significant difference among the groups, $^{*}p < 0.05$, $^{**}p < 0.01$, $^{***}p < 0.001$, $^{****}p < 0.0001$, ns, not significant. WT: wildtype.

SAP deficiency enhances the macrophage infiltration in the periodontium and M1 macrophage polarization during periodontitis

Immunohistochemical results showed the higher infiltration of F4/80 positive macrophages in the periodontium of SAP-KO periodontitis mice compared with wildtype periodontitis mice (Fig. 3a). Quantitative analysis of immunohistochemistry showed a 1.5-fold higher number of macrophages in the periodontal tissue section of SAP-KO periodontitis mice compared with wildtype periodontitis mice (Fig. 3b). A higher number of CD16/32^{+} M1 macrophages were observed in the periodontium of SAP-KO periodontitis mice compared with wildtype periodontitis mice (Fig. 3c-f). Whereas the number of CD206^{+} M2 macrophages was similar in the periodontium of SAP-KO and wildtype mice during periodontitis (Fig. 3d, g). Moreover, LPS-treated BMDM of SAP-KO mice showed 2-fold higher CD86 expression and 3.7-fold lower CD206 expression compared to wildtype mice (Fig. 3h, i). This result indicated that SAP deficiency enhances macrophage infiltration in the periodontium and M1 macrophage polarization during periodontitis.

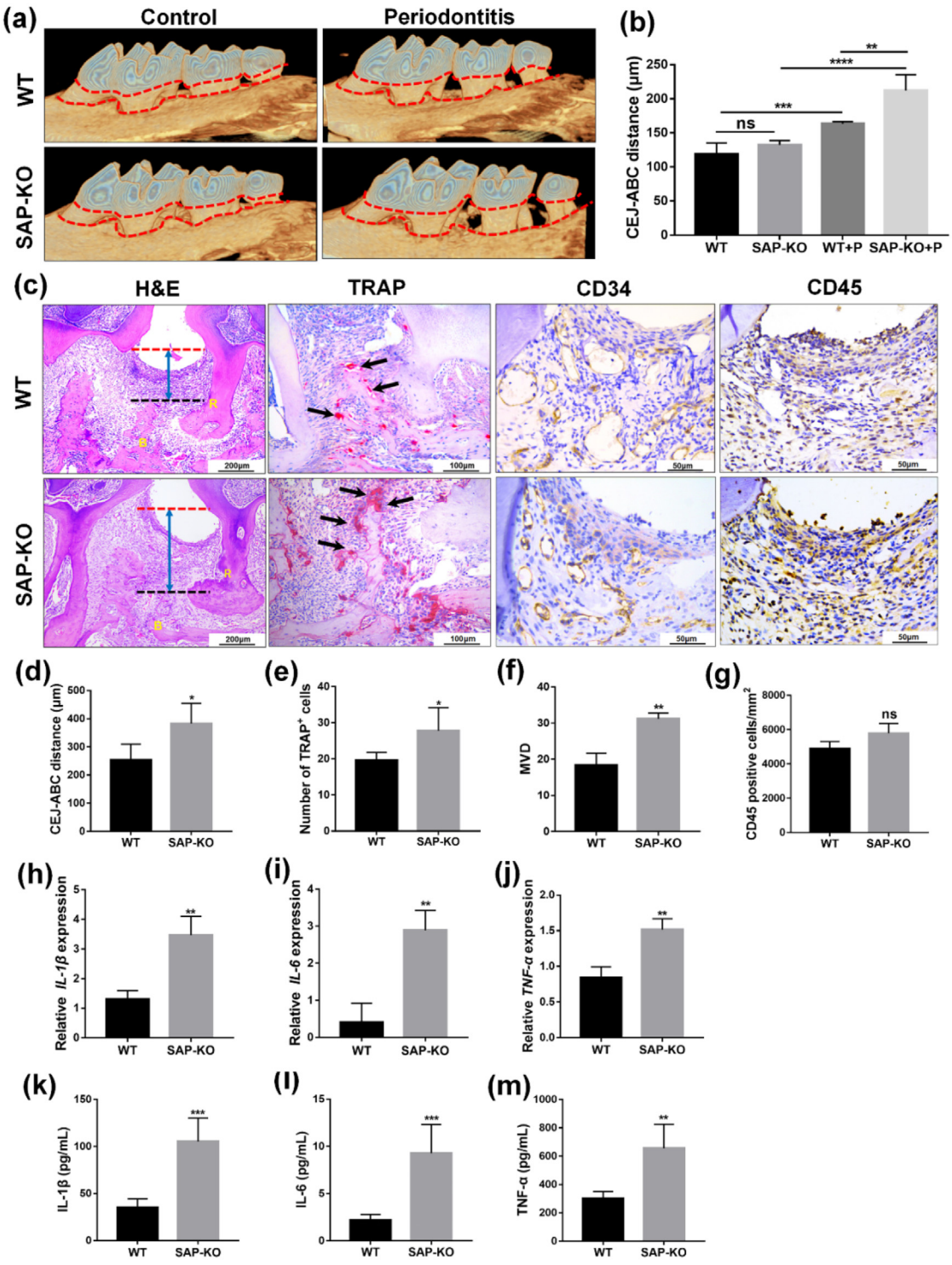

Fig. 2. SAP deficiency aggravates periodontitis and inflammation. (a) Micro-CT 3D reconstruction images of the maxilla of wildtype and SAP-KO mice. (b) CEJ-ABC distance was analyzed from Micro-CT images (n = 5). (c) Histological images of H&E and TRAP staining, and representative CD34 and CD45 immunohistochemistry images of the periodontium in wildtype and SAP-KO periodontitis mice. Quantitative analysis of CEJ-ABC distance (d) and osteoclasts (e) from histological images (n = 5). Quantitative analysis of CD34 (f) and CD45 (g) positive cells from immunohistochemistry images (n = 3). (h-j) Inflammatory cytokine mRNA expression in the periodontium of wildtype and SAP-KO periodontitis mice (n = 3). (k-m) Protein level expression of inflammatory cytokines detected by ELISA (n = 5). Red dot line, CEJ level; Black dot line, ABC level; Blue double arrow line, CEJ-ABC distance. Yellow "R", tooth root; Yellow "B", alveolar bone. Black arrow, osteoclasts. Data are presented as mean ± SD. The significant difference among the groups, $^{*}p < 0.05$, $^{**}p < 0.01$, $^{***}p < 0.001$, ns, not significant. (For interpretation of the references to colour in this figure legend, the reader is referred to the web version of this article.)

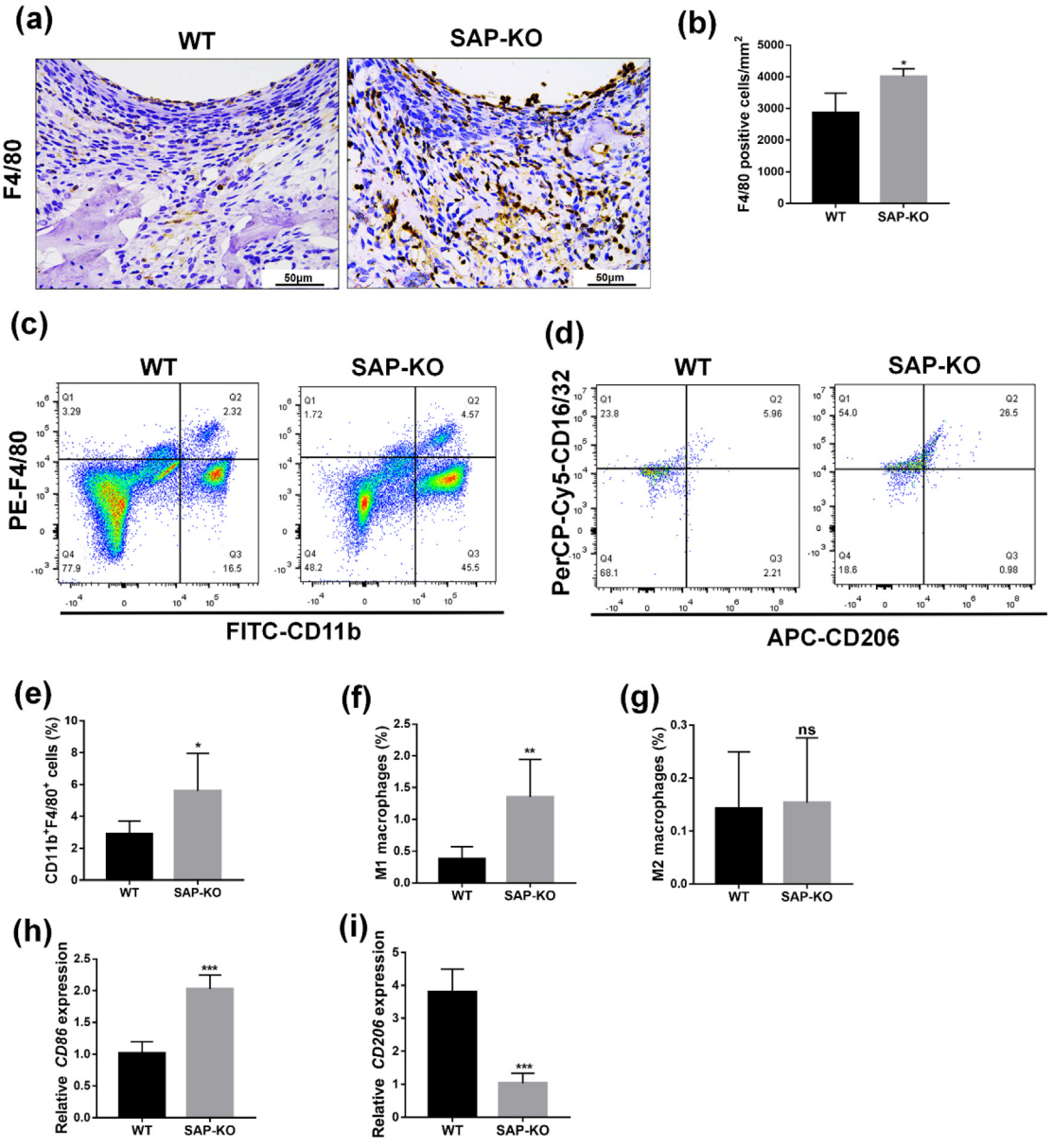

Fig. 3. SAP deficiency enhances the infiltration of macrophages and M1 macrophage polarization in periodontitis. (a) Immunohistochemistry (F4/80) images of periodontium of wildtype mice and SAP-KO periodontitis mice. (b) Quantitative analysis of F4/80 positive cells from immunohistochemistry images (n = 3). FACS images of macrophages sorting using FITC-CD11b and PE-F4/80 (c), CD16/32, and CD206 specific antibody (d). Quantification of the ratio of $CD11b^{+}F4/80^{+}$ (M0 macrophages) (e), $CD16/32^{+}$ (M1 macrophages) cells (f), and $CD206^{+}$ (M2 macrophages) cells (g) from FACS data (n = 7). CD86 (h) and CD206 (i) mRNA expression of LPS-treated BMDM of wildtype and SAP-KO mice (n = 4). Data are presented as mean ± SD. The significant difference among the groups, $^{*}p < 0.05$, $^{**}p < 0.01$, $^{***}p < 0.001$, ns, not significant.

The level of SAP affects oral microbiome homeostasis in periodontitis

Mice oral microbiome abundance and quality in different groups are shown in Fig. S5a. The flattens rarefaction curve indicates sufficient sample sequencing and well-covered sequencing depth. Periodontitis led to a significant difference in alpha diversity of the oral microbiome in both SAP-KO and wildtype mice. As shown in Fig. S5b, Chao 1 indexes of periodontitis groups were lower than those of the healthy control groups. The results showed that the species richness of the SAP-KO and wildtype periodontitis groups was lower than that of the healthy control groups. This result indicates that there is a microbiome imbalance in periodontitis with some dominant bacteria that play a major pathogenic role. Phylum and genus-level differences were observed between bacterial communities from SAP-KO and wildtype periodontitis mice (Fig. 4a, b, c). Specifically, periodontitis increased the abundance of *Porphyromonas* at the genus level in the oral cavity, which is often associated with periodontitis [32]. PCoA of a nonmetric multidimensional scaling plot (on a Bray-Curtis distance matrix) revealed significant qualitative differences in oral microbiota compositions between SAP-KO and wildtype mice (Fig. 4d). Biomarker's analysis using linear discriminant analysis effect size (LEfSe) indicated that the SAP-KO periodontitis mice oral microbiome was characterized by a higher abundance of *Porphyromonas*, *Gemella*, and *Streptococcus_thoraltensis*. Among these, *Porphyromonas* is closely related to periodontitis pathogenicity (Fig. 4e).

SAP-KO significantly promoted periodontitis pathogenicity. Meanwhile, SAP-KO altered oral microbiota during periodontitis with a higher abundance of *Porphyromonas* at the genus level. *P. gingivalis* is the most virulent species of the Porphyromonas genus

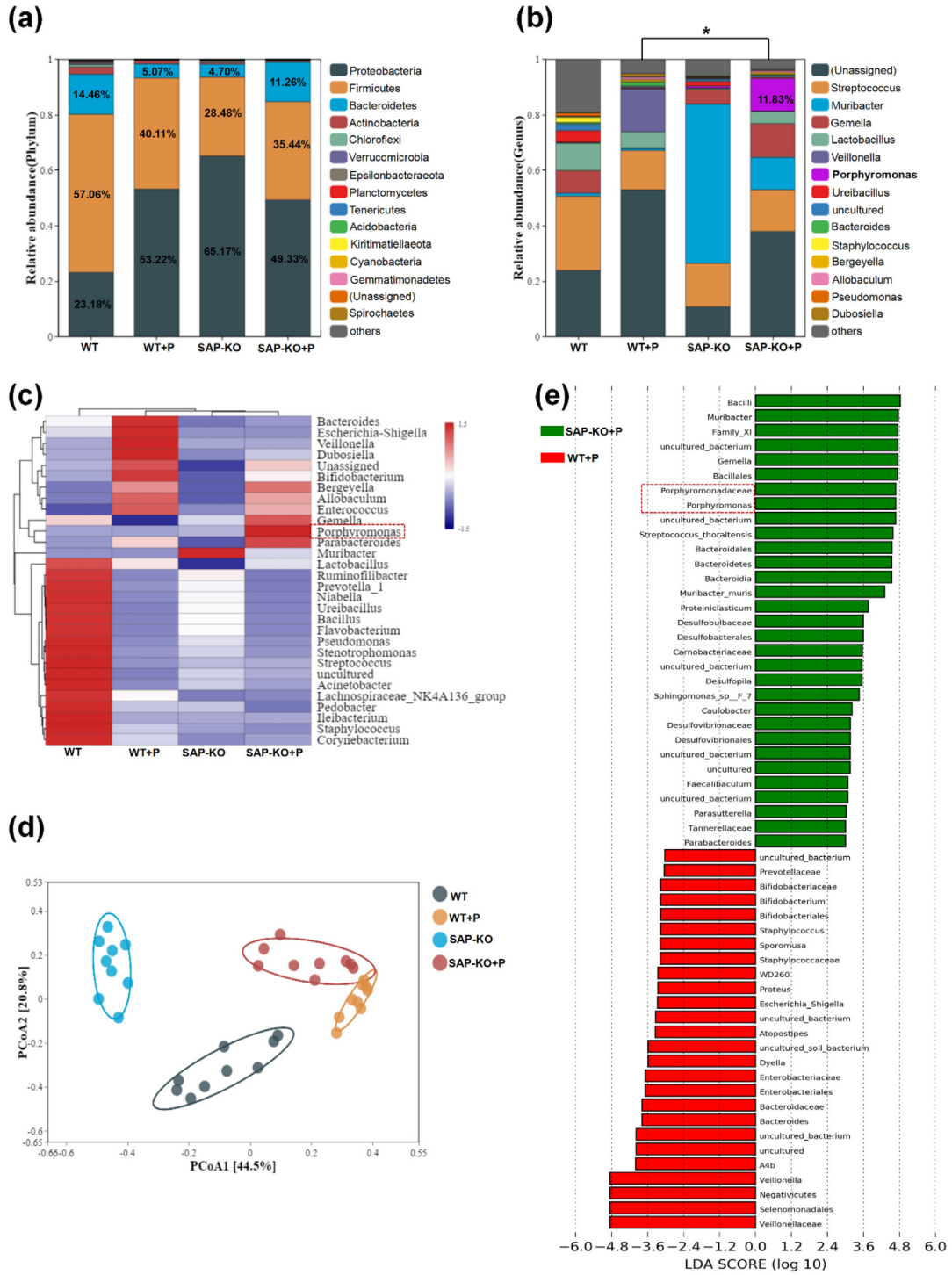

Fig. 4. SAP deficiency alters the oral microbiome in periodontitis. (a) The taxonomic composition of the microbial communities at the phylum level (relative abundance greater than 0.01 % at least one sample (n = 3). (b) The composition of the microbial communities at the genus level There was a statistical difference in the relative abundance of *P. gingivalis* at the genus level. (n = 3). (c) The hierarchical heatmap at the genus level (n = 3). The beta diversity was determined based on the PCoA (d), and LEfSe (e) (n = 3). Data are presented as mean ± SD. The significant difference among the groups, $^{*}p < 0.05$.

involved in human periodontitis pathogenicity. However, the qPCR analysis revealed that there was no expression of *P. gingivalis* in SAP-KO periodontitis mice (data not shown). Based on these facts, we choose human periodontitis-related *P. gingivalis* as a model of Porphyromonas to investigate the role of SAP on macrophage phagocytosis of Porphyromonas during periodontitis.

SAP level regulates macrophage phagocytosis of P. Gingivalis

We further explore the mechanism of higher abundance of *P. gingivalis* in SAP-KO periodontitis mice. Firstly, we analyzed the direct effect of SAP protein in *P. gingivalis* growth. SAP at different concentrations did not affect *P. gingivalis* growth (Fig. S6a). Peri-

odontitis is the result of the interaction between microorganisms and the host's immune system. Macrophages are key immune cells that phagocyte bacteria to eliminate the infection. In SAP-KO periodontitis mice a higher number of macrophages with inflammatory phenotype and a higher abundance of *Porphyromonas* were observed in the periodontium. Therefore, we further analyzed the *P. gingivalis* phagocytosis potential of SAP-KO macrophages.

In the BMDM and *P. gingivalis* co-culture system, phagocytosis of *P. gingivalis* by BMDM was detected by FACS. The FITC (>50 μg/mL) successfully labeled *P. gingivalis* (Fig. S6b). In this experiment, 100 μg/mL FITC was selected for successful labeling of *P. gingivalis*. The macrophage phagocytosis rate of *P. gingivalis* was dramatically reduced in the SAP-KO group compared with the wildtype group at all the time points tested i.e., 30 min, 1 h, and 2 h (Fig. 5a-d). The immunofluorescence staining results of SAP-KO macrophage phagocytosis rate of *P. gingivalis* were consistent with the results of FACS. The reduced *P. gingivalis* phagocytosis by SAP-KO macrophage was further confirmed by immunofluores-

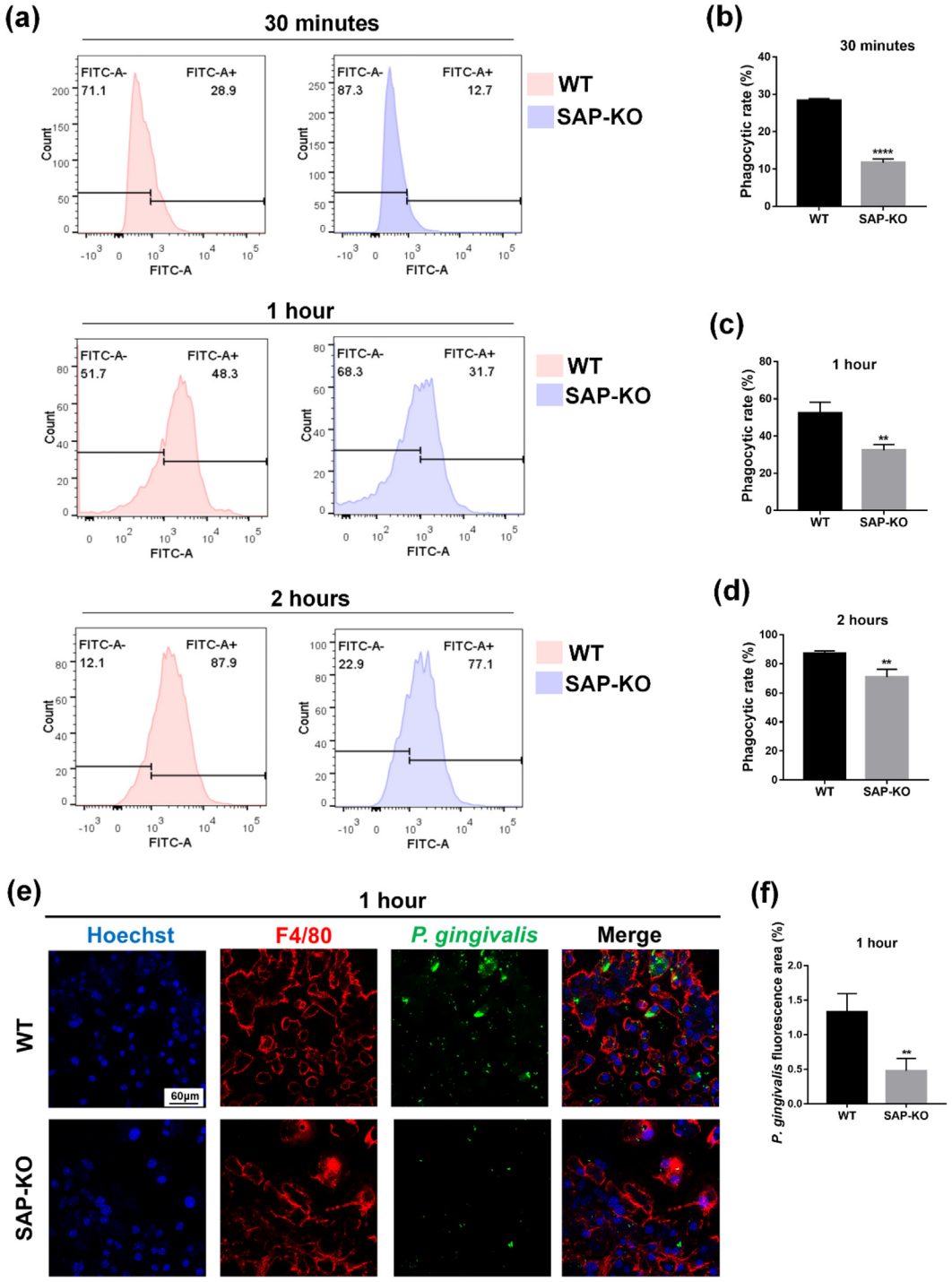

Fig. 5. SAP deficiency inhibits macrophage phagocytosis of *P. gingivalis*. (a) FACS images of phagocytosis of *P. gingivalis* by BMDM. (b-d) Quantitative analysis of phagocytosis rate from FACS analysis (n = 3). (e) Immunofluorescence image of phagocytosis of *P.gingivalis* by BMDM at 1 h. (f) Quantitative analysis of phagocytosis rate from immunofluorescence staining (n = 4). Data are presented as mean ± SD. The significant difference among the groups, $^{**}p < 0.01$, $^{****}p < 0.0001$.

cence staining (Fig. 5e, f; Fig. S6c-f). These results indicate that although the number of macrophages in the periodontium of SAP-KO periodontitis mice was higher, the compromised phagocytosis efficiency causes the higher abundance of *Porphyromonas* in the oral cavity. We further tested the *P. gingivalis* opsonization potential of SAP. There was no effect of SAP-pretreatment of *P. gingivalis* in macrophage recognition and phagocytosis (Fig. S7a-d) indicating no role of SAP on *P. gingivalis* opsonization-mediated macrophage recognition and phagocytosis.

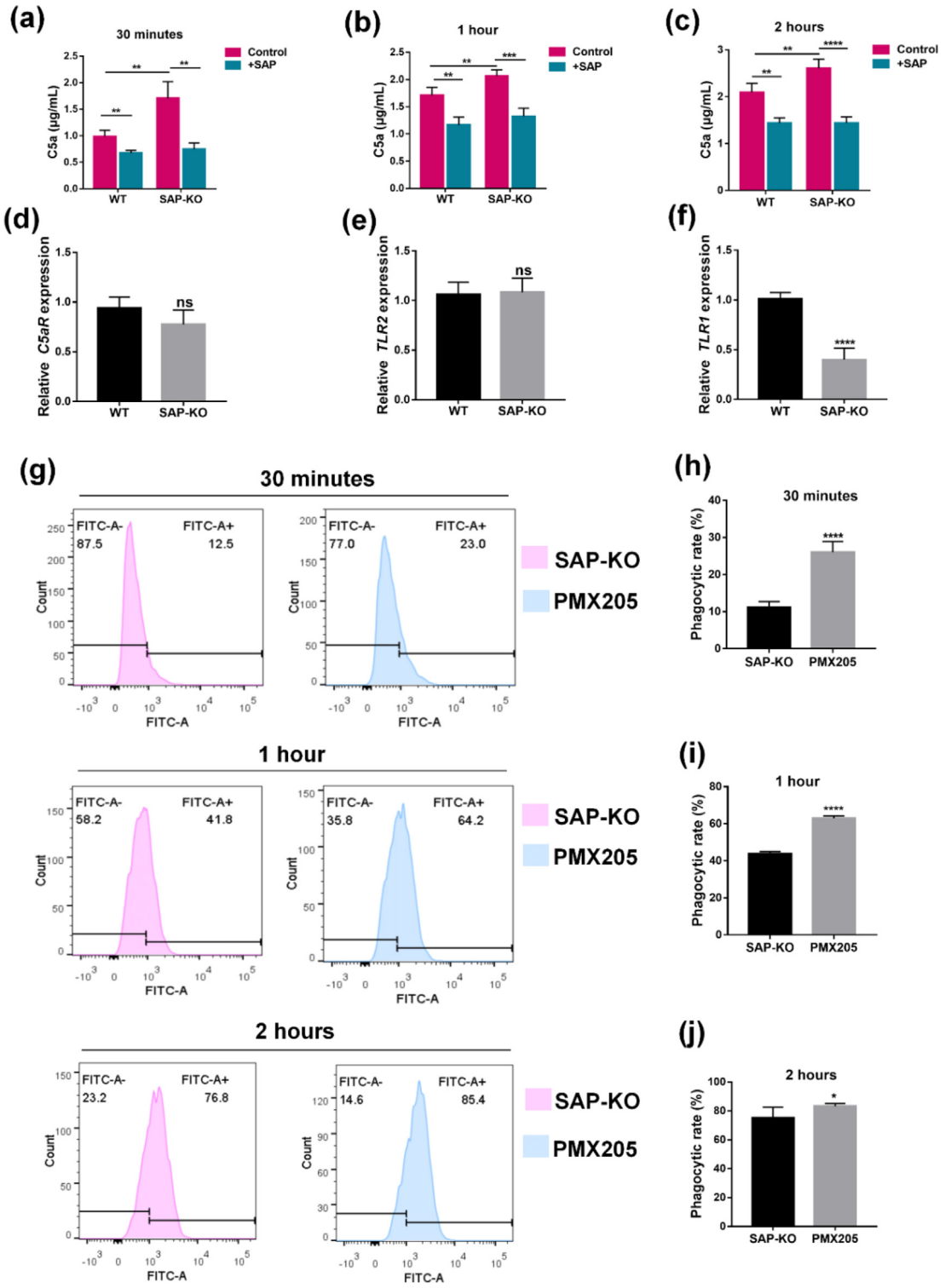

Fig. 6. SAP deficiency inhibits macrophage phagocytosis of *P. gingivalis* by activating the C5a-C5aR pathway. Expression of C5a in *P.gingivalis* and BMDM co-culture for 30 min (a), 1 h (b), and 2 h (c), respectively (n = 4). Quantitative PCR analysis of C5aR (d), TLR2 (e), and TLR1 (f) mRNA expression in BMDM (n = 6). (g) FACS images of phagocytosis of *P. gingivalis* by BMDM of SAP-KO mice with or without PMX205. (h-j) Quantitative analysis of phagocytosis rate (n = 5). Data are presented as mean ± SD. The significant difference among the groups, $^{*}p < 0.05$, $^{**}p < 0.01$, $^{***}p < 0.001$, $^{****}p < 0.0001$, ns, not significant.

SAP deficiency inhibits macrophage phagocytosis of P. gingivalis by activating the C5a-C5aR pathway

Studies have shown that *P. gingivalis* releases active C5a fragments from C5 complement via its Arg-specific gingipains [24]. The binding of C5a and macrophage C5aR crosstalks with TLR2 to inhibit the phagocytosis of *P. gingivalis* [5,23]. Therefore, we tested the effect of SAP deficiency in C5a release from *P. gingivalis*. The ELISA results showed that SAP-KO macrophages dramatically increased the C5a expression by *P. gingivalis* at 30 min, 1 h, and 2 h of co-culture. However, when recombinant SAP protein was added to the co-culture system, the expression level of C5a decreased in both wildtype and SAP-KO macrophages (Fig. 6a-c). Next, we investigated the expression of C5aR and TLR2/1 on macrophages from SAP-KO and wildtype mice in the co-culture system. There was no significant difference in the expression of C5aR and TLR2 in macrophages of SAP-KO mice and wildtype mice. These results indicate that SAP-KO did not directly affect the content of C5aR-TLR2 in macrophages to inhibit the macrophage phagocytosis of *P. gingivalis* (Fig. 6d-f). Finally, PMX205, an antagonist of C5a, was added to the co-culture system to further validate our results. The experiment showed that phagocytosis of *P. gingivalis* by SAP-KO macrophage robustly improved after blocking C5a-C5aR signaling by PMX205 (Fig. 6g-j). Therefore, our results demonstrate that SAP deficiency inhibits macrophage phagocytosis of *P. gingivalis* via inducing C5a release by *P. gingivalis* and activation of C5a-C5aR signaling in macrophages.

Discussion

Periodontitis is mainly caused by oral microbiome dysbiosis and host immune responses [2]. SAP is a pattern recognition molecule that modulates bacterial infections and inflammation in various diseases [33–35]. However, the level of SAP in periodontal tissue and its role in periodontitis pathogenicity is still unknown. In this study, we found that macrophage-specific SAP was the main source of the elevated level of SAP in the periodontium of periodontitis patients and mice. SAP-KO mice displayed more severe periodontitis and inflammation as well as infiltration of a higher number of macrophages with M1 phenotype in the periodontium. SAP-KO periodontitis mice exhibited a disturbed oral microbiome with a higher abundance of *Porphyromonas* at the genus level. SAP-KO macrophages induced C5a release from *P. gingivalis* and inhibited macrophage phagocytosis of *P. gingivalis* via C5a-C5aR signaling. This explains the possible mechanism of a higher abundance of *Porphyromonas* in the oral cavity of SAP-KO periodontitis mice. A higher number of M1 macrophages with compromised phagocytosis of *Porphyromonas* could be the reason behind the aggravated periodontitis in SAP-KO mice. Our results suggest the possible protective role of elevated levels of SAP in periodontal macrophages against periodontitis progression.

SAP and c-reactive protein (CRP) are the classical short-arm pentraxins that play a role in innate immunity and inflammatory diseases. CRP has been widely applied as a diagnostic and prognostic marker in clinical practice [36,37]. According to the reports from the literature, CRP is associated with periodontitis [38,39]. SAP has been studied as a potential therapeutic agent to treat immune or inflammatory diseases. Injection of exogenous SAP protein inhibits systemic lupus erythematosus and radiation-induced oral mucositis in mice [40,41]. Phase II clinical trials showed that injection of human recombinant SAP protein partially reverses pulmonary fibrosis and improves lung function [42,43]. While the level of SAP in different tissues during periodontitis has not been investigated yet. According to previous studies and the data from Human Protein Atlas, SAP is secreted mainly by hepatocytes in the liver and circulates in blood [20]. However, the SAP level in periodontium during periodontitis and its role in periodontitis pathogenicity has not been investigated yet. The level of SAP in gingival tissue from periodontitis patients was 4-fold higher compared with the healthy individuals. A similar pattern of SAP level was found in periodontium and gingiva of periodontitis mice. Interestingly, SAP levels in the liver and blood remained unchanged in periodontitis mice compared with control mice. These results indicate local overexpression of SAP in periodontium rather than in the liver during periodontitis. We further explored the expression of SAP in different cell types present in the periodontium. Only macrophages but not the osteoblasts and GECs showed higher SAP expression during inflammatory conditions. Overexpression of SAP in macrophages during periodontitis further supports the role of macrophages in periodontitis pathogenicity. These findings provide the basis for in-depth research on the role of SAP in periodontitis.

Micro-CT and H&E staining results showed that periodontitis aggravates alveolar bone resorption in SAP-KO periodontitis mice compared with wildtype. Increased osteoclast number and inflammation in periodonttis cause alveolar bone loss [44,45]. Several studies have reported a higher microvasculature and leucocyte infiltration in gingival tissues of severe periodontitis cases [46–48]. SAP-KO periodontitis mice showed a robustly higher number of osteoclasts, microvasculature, immune cells' infiltration, and M1 macrophages in the periodontium compared with the wildtype periodontitis mice. Similarly, the levels of pro-inflammatory cytokines IL-1β, IL-6, and TNF-α were remarkably higher in the periodontium of SAP-KO periodontitis mice compared with wildtype periodontitis mice. M1 macrophages release pro-inflammatory cytokines that activate Th17 cells to produce IL-17, IL-1, IL-6, TNF-α, MMP-9, and RANKL [19,49]. These proinflammatory factors had been reported to promote osteoclast formation and activity, resulting in higher alveolar bone resorption during periodontitis [50,51]. Moreover, SAP had been reported to attenuate M2 macrophage (anti-inflammatory) polarization during fungal infection of the respiratory tract [21]. We found a similar level of M2 macrophage marker CD206 expression in the periodontium of SAP-KO and wildtype periodontitis mice. However, CD206 expression was dramatically downregulated in LPS-treated BMDMs from SAP-KO mice compared to that of wildtype mice. This discrepancy in results of in vitro and in vivo studies might be related to the differences in cell origin, complex periodontitis milieu in vivo, and the high standard deviation of the in vivo results. The results from the literature and current study indicate that a higher number of M1 macrophages in the periodontium of SAP-KO periodontitis mice could be a possible factor aggravating periodontitis pathogenicity.

SAP regulates bacterial virulence and host immune cells function differentially in a bacteria and disease-specific manner [34,52]. In this study, SAP-KO altered the oral microbiome of periodontitis mice with the most significant abundance of *Porphyromonas* at the genus level and the lower abundance of the overall oral microbiome. A higher abundance of *P. gingivalis* alters the numbers and composition of symbiotic bacteria to low abundance resulting in oral microbial dysbiosis and periodontitis [53,54]. We further analyzed *P. gingivalis* recognition and phagocytosis efficiency of SAP-KO macrophages. Our results indicated that the higher abundance of *Porphyromonas* in the periodontium of SAP-KO periodontitis mice is related to the compromised recognition and phagocytosis of *P. gingivalis* by SAP-KO macrophages. Our results indicate the regulatory role of SAP in host immune cell-mediated recognition and phagocytosis of oral pathogenic bacteria. Based on these results we assume that compromised bacterial recognition and phagocytosis by SAP-KO macrophages result in a higher abundance of *Porphyromonas* in the oral cavity, which could

further cause oral microbiome dysbiosis. The dysbiotic pathogenic oral microbiome induces infiltration of macrophages in the periodontium and M1 polarization triggering a higher degree of inflammation that could exacerbate periodontitis pathogenicity in SAP-KO mice.

Exogenous SAP did not affect *P. gingivalis* growth and opsonization. Studies have shown that *P. gingivalis* releases active C5a fragments from C5 complement via its Arg-specific gingipains [32,55,56]. The C5a binds with C5aR of phagocytic cells and crosstalk with TLR2, inhibiting the phagocytosis of *P. gingivalis* [5,23,25]. C5a is a key molecule for *P. gingivalis* to escape immune clearance and induce inflammation [57–59]. Interestingly, *P. gingivalis* co-cultured with SAP-KO macrophages showed a higher expression of C5a. Exogenous SAP treatment successfully reduced the C5a expression by *P. gingivalis* co-cultured with macrophages from wildtype and SAP-KO mice. Furthermore antagonizing C5a-C5aR signaling robustly promoted the recognition and phagocytosis of *P. gingivalis* by SAP-KO macrophages. However, *P. gingivalis* co-culture with SAP-KO macrophages did not alter the expression of C5aR and TLR2 in SAP-KO macrophages. These results indicate that during SAP-deficiency *P. gingivalis* releases a higher level of C5a activating C5a-C5aR signaling in macrophages which inhibits the phagocytosis of *P. gingivalis* causing its' abundance in the oral cavity. However, the mechanism of SAP deficiency-mediated higher expression of C5a in *P. gingivalis* should be further studied. Moreover, our findings should be further verified in SAP-Tg periodontitis mice.

Conclusions

This study unraveled upregulated SAP in the periodontium macrophages during periodontitis. Interestingly, SAP-KO resulted in oral microbiome dysbiosis with a higher abundance of *Porphyromonas* at the genus level and aggravated inflammation, infiltration of M1 macrophages, osteoclast numbers, and periodontitis pathogenicity. SAP deficiency-induced C5a release from *P. gingivalis* activated C5a-C5aR signaling in macrophages to inhibit the phagocytosis of *P. gingivalis*. Based on our results, the higher level of periodontal SAP during periodontitis could have a protective role against disease.

Compliance with Ethics Requirements

All Institutional and National Guidelines for the care and use of animals (fisheries) were followed.

All procedures followed were in accordance with the ethical standards of the responsible committee on human experimentation (institutional and national) and with the Helsinki Declaration of 1975, as revised in 2008 (5). Informed consent was obtained from all patients for being included in the study.

CRediT authorship contribution statement

Liping Wang: Conceptualization, Data curation, and Writing – original draft. **Dongliang Liang:** Conceptualization, Data curation, and Writing – original draft. **Yinyin Huang:** Conceptualization, Data curation, and Writing – original draft. **Yunxin Chen:** Investigation, Methodology, Formal analysis, and Software interpreted data. **Xiaocong Yang:** Investigation, Methodology, Formal analysis, and Software interpreted data. **Zhijun Huang:** Investigation, Methodology, Formal analysis, and Software interpreted data. **Yiqin Jiang:** Investigation, Methodology, Formal analysis, and Software interpreted data. **Hanfu Su:** Investigation, Methodology, Formal analysis, and Software interpreted data. **Lijing Wang:** Conceptualization, Funding acquisition, Supervision, Validation, and Writing – review & editing. **Janak Lal Pathak:** Conceptualization, Funding acquisition, Supervision, Validation, and Writing – review & editing. **Linhu Ge:** Conceptualization, Funding acquisition, Supervision, Validation, and Writing – review & editing.

Declaration of Competing Interest

The authors declare that they have no known competing financial interests or personal relationships that could have appeared to influence the work reported in this paper.

Acknowledgments

This study was supported by the National Natural Science Foundation of China (82150410451), the Basic and Applied Basic Research Foundation of Guangdong Province (2021A1515110988), the project of Guangzhou Science and Technology Bureau (202002030301), Guangzhou City Clinical Key Speciality Cultivation Project (2021115257) and High-level university construction funding of Guangzhou Medical University (02-410-B205001293, B195002003017, 02-412-B205002-1003017, and 06-410-2106035).

Appendix A. Supplementary material

Supplementary data to this article can be found online at https://doi.org/10.1016/j.jare.2022.10.003.

References

[1] Hajishengallis G, Korostoff JM. Revisiting the page & schroeder model: The good, the bad and the unknowns in the periodontal host response 40 years later. Periodontology 2000;2017(75):116–51.
[2] Hajishengallis G. Periodontitis: From microbial immune subversion to systemic inflammation. Nat Rev Immunol 2015;15(1):30–44.
[3] Lamont RJ, Hajishengallis G. Polymicrobial synergy and dysbiosis in inflammatory disease. Trends Mol Med 2015;21(3):172–83.
[4] Matsha TE, Prince Y, Davids S, Chikte U, Erasmus RT, Kengne AP, et al. Oral microbiome signatures in diabetes mellitus and periodontal disease. J Dent Res 2020;99(6):658–65.
[5] Hajishengallis G, Darveau RP, Curtis MA. The keystone-pathogen hypothesis. Nature reviews. Microbiology 2012;10(10):717–25.
[6] Takeuchi H, Sasaki N, Yamaga S, Kuboniwa M, Matsusaki M, Amano A, et al. Porphyromonas gingivalis induces penetration of lipopolysaccharide and peptidoglycan through the gingival epithelium via degradation of junctional adhesion molecule 1. PLoS Pathog 2019;15(11):e1008124.
[7] Cathcart ES, Comerford FR, Cohen AS. Immunologic studies on a protein extracted from human secondary amyloid. N Engl J Med 1965;273(3):143–6.
[8] Lech M, Rommele C, Anders HJ. Pentraxins in nephrology: C-reactive protein, serum amyloid p and pentraxin-3. Nephrology, Dial, Transplant: Off Publ Eur Dial Transplant Assoc – Eur Renal Assoc 2013;28:803–11.
[9] Ochrietor JD, Harrison KA, Zahedi K, Mortensen RF. Role of stat3 and c/ebp in cytokine-dependent expression of the mouse serum amyloid p-component (sap) and c-reactive protein (crp) genes. Cytokine 2000;12(7):888–99.
[10] Poulsen ET, Pedersen KW, Marzeda AM, Enghild JJ. Serum amyloid p component (sap) interactome in human plasma containing physiological calcium levels. Biochemistry 2017;56(6):896–902.
[11] Pepys MB, Baltz MARILYN, Gomer K, Davies AJS, Doenhoff M. Serum amyloid p-component is an acute-phase reactant in the mouse. Nature 1979;278 (5701):259–61.
[12] Bottazzi B, Inforzato A, Messa M, Barbagallo M, Magrini E, Garlanda C, et al. The pentraxins ptx3 and sap in innate immunity, regulation of inflammation and tissue remodelling. J Hepatol 2016;64(6):1416–27.
[13] Noursadeghi M, Bickerstaff MCM, Gallimore JR, Herbert J, Cohen J, Pepys MB. Role of serum amyloid p component in bacterial infection: Protection of the host or protection of the pathogen. Proc Natl Acad Sci USA 2000;97 (26):14584–9.
[14] Behrens NE, Lipke PN, Pilling D, Gomer RH, Klotz SA, Lorenz M, et al. Serum amyloid p component binds fungal surface amyloid and decreases human macrophage phagocytosis and secretion of inflammatory cytokines. mBio 2019;10(2).
[15] An J-H, Kurokawa K, Jung D-J, Kim M-J, Kim C-H, Fujimoto Y, et al. Human sap is a novel peptidoglycan recognition protein that induces complement-independent phagocytosis of staphylococcus aureus. J Immunol (Baltimore, Md: 1950) 2013;191(6):3319–27.

[16] Short LL, Zoellner H, Hunter N. Association of amyloid p protein with pathology in periodontal tissues. J Oral Pathol Med: Off Publ Int Assoc Oral Pathol Am Acad Oral Pathol 1994;23(8):354–7.
[17] Yang J, Zhu Y, Duan D, Wang P, Xin Y, Bai L, et al. Enhanced activity of macrophage m1/m2 phenotypes in periodontitis. Arch Oral Biol 2018;96:234–42.
[18] Betancur D, Muñoz Grez C, Oñate A. Comparative analysis of cytokine expression in oral keratinocytes and thp-1 macrophages in response to the most prevalent serotypes of aggregatibacter actinomycetemcomitans. Microorganisms 2021;9(3):622.
[19] Sima C, Glogauer M. Macrophage subsets and osteoimmunology: Tuning of the immunological recognition and effector systems that maintain alveolar bone. Periodontology 2000;2013(63):80–101.
[20] Cox N, Pilling D, Gomer RH. Serum amyloid p: A systemic regulator of the innate immune response. J Leukoc Biol 2014;96(5):739–43.
[21] Moreira AP, Cavassani KA, Hullinger R, Rosada RS, Fong DJ, Murray L, et al. Serum amyloid p attenuates m2 macrophage activation and protects against fungal spore-induced allergic airway disease. J Allergy Clin Immunol 2010;126 (4):712–721.e7.
[22] Pilling D, Gomer RH. The development of serum amyloid p as a possible therapeutic. Front Immunol 2018;9.
[23] Wang M, Krauss JL, Domon H, Hosur KB, Liang S, Magotti P, et al. Microbial hijacking of complement-toll-like receptor crosstalk. Sci Signaling 2010;3 (109).
[24] Liang S, Krauss JL, Domon H, McIntosh ML, Hosur KB, Qu H, et al. The c5a receptor impairs il-12-dependent clearance of porphyromonas gingivalis and is required for induction of periodontal bone loss. J Immunol (Baltimore, Md: 1950) 2011;186(2):869–77.
[25] Hajishengallis G, Abe T, Maekawa T, Hajishengallis E, Lambris JD. Role of complement in host-microbe homeostasis of the periodontium. Semin Immunol 2013;25(1):65–72.
[26] Liu M, Mu H, Peng W, Zhao L, Hu W, Jiang Z, et al. Time-dependent c5a and c5ar expression in dental pulp cells following stimulation with lta and lps. Int J Mol Med 2019.
[27] Haag S, Murthy A. Murine Monocyte and Macrophage Culture. Bio-protocol 2021;11(6):e3928.
[28] Abe T, Hajishengallis G. Optimization of the ligature-induced periodontitis model in mice. J Immunol Methods 2013;394(1-2):49–54.
[29] Marchesan J, Girnary MS, Jing Li, Miao MZ, Zhang S, Sun Lu, et al. An experimental murine model to study periodontitis. Nat Protoc 2018;13 (10):2247–67.
[30] Pathak JL, Fang Y, Chen Y, et al. Downregulation of macrophage-specific act-1 intensifies periodontitis and alveolar bone loss possibly via tnf/nf-κb signaling. Front Cell Dev Biol 2021;9:628139.
[31] Wang L, Zheng J, Pathak JL, et al. Slit2 overexpression in periodontitis intensifies inflammation and alveolar bone loss, possibly via the activation of mapk pathway. Front Cell Dev Biol 2020;8:593.
[32] Jia L, Han N, Du J, et al. Pathogenesis of important virulence factors of porphyromonas gingivalis via toll-like receptors. Front Cell Infect Microbiol 2019;9:262.
[33] Shi YH, Chen K, Ma WJ, et al. Ayu c-reactive protein/serum amyloid p agglutinates bacteria and inhibits complement-mediated opsonophagocytosis by monocytes/macrophages. Fish Shellfish Immunol 2018;76:58–67.
[34] Tsutsui S, Matsui S, Nakamura O. Serum amyloid p-component/c-reactive proteins in fugu (takifugu rubripes) egg with binding ability to disease-causing bacteria by carbohydrate-recognition. Dev Comp Immunol 2020;111:103748.
[35] Wang T, Sun L. Cssap, a teleost serum amyloid p component, interacts with bacteria, promotes phagocytosis, and enhances host resistance against bacterial and viral infection. Dev Comp Immunol 2016;55:12–20.
[36] Casas JP, Shah T, Hingorani AD, et al. C-reactive protein and coronary heart disease: A critical review. J Intern Med 2008;264:295–314.
[37] Deme D, Telekes A. prognostic importance of plasma c-reactive protein (crp) in oncology. Orv Hetil 2017;158:243–56.
[38] Sun XJ, Meng HX, Shi D, et al. Elevation of c-reactive protein and interleukin-6 in plasma of patients with aggressive periodontitis. J Periodontal Res 2009;44:311–6.
[39] Gomes-Filho IS, Freitas Coelho JM, da Cruz SS, et al. Chronic periodontitis and c-reactive protein levels. J Periodontol 2011;82:969–78.
[40] Murray LA, Kramer MS, Hesson DP, et al. Serum amyloid p ameliorates radiation-induced oral mucositis and fibrosis. Fibrogenesis Tissue Repair 2010;3:11.
[41] Zhang W, Xu W, Xiong S. Macrophage differentiation and polarization via phosphatidylinositol 3-kinase/akt-erk signaling pathway conferred by serum amyloid p component. J Immunol (Baltimore, Md: 1950) 2011;187:1764–77.
[42] Dillingh MR, van den Blink B, Moerland M, et al. Recombinant human serum amyloid p in healthy volunteers and patients with pulmonary fibrosis. Pulm Pharmacol Ther 2013;26:672–6.
[43] Raghu G, van den Blink B, Hamblin MJ, et al. Effect of recombinant human pentraxin 2 vs placebo on change in forced vital capacity in patients with idiopathic pulmonary fibrosis: A randomized clinical trial. JAMA 2018;319:2299–307.
[44] Kitaura H, Marahleh A, Ohori F, et al. Osteocyte-related cytokines regulate osteoclast formation and bone resorption. Int J Mol Sci 2020;21.
[45] Hienz SA, Paliwal S, Ivanovski S. Mechanisms of bone resorption in periodontitis. J Immunol Res 2015;2015:615486.
[46] Kasprzak A, Surdacka A, Tomczak M, et al. Expression of angiogenesis-stimulating factors (vegf, cd31, cd105) and angiogenetic index in gingivae of patients with chronic periodontitis. Folia Histochem Cytobiol 2012;50:554–64.
[47] Kasprzak A, Surdacka A, Tomczak M, et al. Role of high endothelial postcapillary venules and selected adhesion molecules in periodontal diseases: A review. J Periodontal Res 2013;48:1–21.
[48] Wu YH, Kuraji R, Taya Y, et al. Effects of theaflavins on tissue inflammation and bone resorption on experimental periodontitis in rats. J Periodontal Res 2018;53:1009–19.
[49] Shapouri-Moghaddam A, Mohammadian S, Vazini H, et al. Macrophage plasticity, polarization, and function in health and disease. J Cell Physiol 2018;233:6425–40.
[50] Cardoso EM, Reis C, Manzanares-Céspedes MC. Chronic periodontitis, inflammatory cytokines, and interrelationship with other chronic diseases. Postgrad Med 2018;130:98–104.
[51] Li Y, Ling J, Jiang Q. Inflammasomes in alveolar bone loss. Front Immunol 2021;12:691013.
[52] Noursadeghi M, Bickerstaff MC, Gallimore JR, et al. Role of serum amyloid p component in bacterial infection: Protection of the host or protection of the pathogen. Proc Natl Acad Sci USA 2000;97:14584–9.
[53] Olsen I, Lambris JD, Hajishengallis G. Porphyromonas gingivalis disturbs host-commensal homeostasis by changing complement function. J Oral Microbiol 2017;9:1340085.
[54] Darveau RP, Hajishengallis G, Curtis MA. Porphyromonas gingivalis as a potential community activist for disease. J Dent Res 2012;91:816–20.
[55] Hajishengallis G, Liang S, Payne MA, et al. Low-abundance biofilm species orchestrates inflammatory periodontal disease through the commensal microbiota and complement. Cell Host Microbe 2011;10:497–506.
[56] Wingrove JA, DiScipio RG, Chen Z, et al. Activation of complement components c3 and c5 by a cysteine proteinase (gingipain-1) from porphyromonas (bacteroides) gingivalis. J Biol Chem 1992;267:18902–7.
[57] Munenaga S, Ouhara K, Hamamoto Y, et al. The involvement of c5a in the progression of experimental arthritis with porphyromonas gingivalis infection in skg mice. Arthritis Res Therapy 2018;20:247.
[58] Hajishengallis G, Krauss JL, Jotwani R, et al. Differential capacity for complement receptor-mediated immune evasion by porphyromonas gingivalis depending on the type of innate leukocyte. Mol Oral Microbiol 2017;32:154–65.
[59] Hajishengallis G. Immune evasion strategies of porphyromonas gingivalis. J Oral Biosci 2011;53:233–40.